Adaptive Brownian Dynamics Simulation for Estimating Potential Mean Force in Ion Channel Permeation

Vikram Krishnamurthy*, *Fellow, IEEE*, and Shin-Ho Chung

***Abstract*—Ion channels are biological nanotubes formed by large protein molecules in the cell membrane. This paper presents a novel multiparticle simulation methodology, which we call adaptive controlled Brownian dynamics, for estimating the force experienced by a permeating ion at each discrete position along the ion-conducting pathway. The profile of this force, commonly known as the *potential of mean force*, results from the electrostatic interactions between the ions in the conduit and all the charges carried by atoms forming the channel the protein, as well as the induced charges on the protein wall. The current across the channel is solely determined by the potential of mean force encountered by the permeant ions. The simulation algorithm yields consistent estimates of this profile. The algorithm operates on an angstrom unit spatial scale and femtosecond time scale. Numerical simulations on the gramicidin ion channel show that the algorithm yields the potential of mean force profile that accurately reproduces experimental observations.**

***Index Terms*—Brownian dynamics, Gramicidin, ion channel, ion permeation, potential mean force, stochastic optimization.**

I. Introduction

ALL living cells are surrounded by a cell membrane, composed of two layers of phospholipid molecules, called the lipid bilayer. Ion channels are water-filled pores formed by large protein molecules in the cell membrane. These pores are *protein nanotubes* that permit the diffusion of ions across the cell membrane into or out of the cell. Although we use the term protein nanotube, ion channels are typically the size of angstrom units $(10^{-10}$ m), i.e., an order of magnitude smaller in radius and length compared to carbon nanotubes that are used in nanodevices. All electrical activities in the nervous system, including communications between cells and the influence of hormones and drugs on cell function, are regulated by ion channels. Therefore, understanding their mechanisms and structure at a molecular level is a fundamental problem in biology.

The setting of this paper is the so-called permeation problem in ion channels [1], [2]. The permeation problem seeks to explain the working of an ion channel at an Å spatial scale by studying the propagation of individual ions through the ion channel at a femto (10^{-15})-second time scale. This setup is said to be at a *mesoscopic scale*, since the individual ions (e.g., Na^+ ions which are 0.95 Å in radius) are comparable in radius to the nanotube. At this mesoscopic level, point charge approximations and continuum electrostatics break down for narrow ion channels such as gramicidin-A ion channels. The discrete finite nature of each ion needs to be taken into consideration. Also, failure of the mean field approximation in narrow ion channels implies that any theory that aspires to relate ion channel structure to its function must treat ions explicitly [3].

The aim of this paper is to estimate the profile of the force experienced by the ion traversing the pore such that the simulated ion channel current using *mesoscopic Brownian dynamics simulations* matches experimentally measured channel currents under various conditions. In the mesoscopic Brownian dynamics simulation of an ion channel, an interacting multiparticle system of ions is simulated where the dynamics of each individual ion follows Langevin's stochastic differential equation [4]. As a result of the external applied potential to the ion channel and the charges of the atoms in the protein lining the inner wall of the nanotube, there is a drift of ions from outside to inside the cell via the ion channel resulting in the simulated current. For each ion that enters the protein nanotube, the force experienced by the ion is a function of the charges of the atoms lining the inner wall of the nanotube. Thus, the mean passage time for an ion to traverse the nanotube and hence the simulated ion channel current is a function of the structure of the atoms lining the nanotube. By optimizing the fit between the Brownian dynamics simulated current with experimentally observed ion channel currents, one can then estimate the charges of the atoms lining the nanotube. The main idea of this paper is to formulate this stochastic optimization problem and present a provably convergent adaptive algorithm that controls the behavior of the large scale multiparticle Brownian dynamics simulation to estimate the effective charge structure.

The effective charge structure of the atoms lining the nanotube is conveniently summarized by the potential of mean force (PMF) which comprises electrostatic forces acting on each ion when it is in or near the ion channel. Our aim is to estimate the PMF profile of the ion channel, i.e., how the PMF varies along the length of the nanotube at an Å spatial resolution. Determining the PMF profile that optimizes the fit between the mesoscopic simulated current and observed current yields useful information and insight into how an ion channel works at a mesoscopic level. Determining the optimal PMF profile is important for several reasons. First, it yields the effective charge density in the peptides that form the ion channel. Second, for theoretical biophysicists, the PMF profile

Manuscript received May 23, 2005; revised December 22, 2005. This work was supported by the Natural Sciences and Engineering Research Council of Canada (NSERC). *Asterisk indicates corresponding author.*

*V. Krishnamurthy is with the Department of Electrical and Computer Engineering, University of British Columbia, Vancouver V6T 1Z4, Canada (e-mail: vikramk@ece.ubc.ca).

S. H. Chung is with the Department of Biophysics, Australian National University, Canberra, ACT 0200, Australia (e-mail: shin-ho.chung@anu.edu.au).

Digital Object Identifier 10.1109/TNB.2006.875035

yields information about the permeation dynamics including the locations of *binding sites* where the ions in the channel are likely to be trapped, the mean velocity of propagation of ions through the channel and the conductance of the ion channel.

A. Main Results

The method of adaptive controlled Brownian dynamics we propose in this paper is designed to circumvent the limitations posed on the conventional Brownian dynamics simulation approach. Conventionally, the electrostatic force experienced by an ion attempting to traverse the pore is first calculated by solving Poisson's equation, which requires a prior knowledge of the channel structure, the charge state of each ionizable residue, and the dielectric constants of the protein and the pore. In the learning-based dynamic control algorithm proposed here, we solve the inverse problem. That is, given the three-dimensional (3-D) shape of an ion channel, we deduce the PMF encountered by an ion traversing the channel that correctly replicate experimental findings. To achieve this aim, we first make an initial guess of the PMF, representing it with a Gaussian mixture basis function or other basis function, characterized by a multidimensional parameter vector, and then successively refine the initial guess using a stationary stochastic optimization algorithm. In this way, we derive the PMF that minimizes the mean square error between the simulated current and the actual observed experimental current.

The main results of this paper are as follows.

1) To set the stage for devising the adaptive controlled Brownian dynamics algorithms proposed in this paper, we first provide a mathematically complete formulation and statistical analysis of the Brownian dynamics simulation for tracing the trajectories of ions across the protein nanotube. This mathematical formalism is essential to devise a statistically consistent adaptive Brownian dynamics algorithm. We give a complete formulation of the permeation of ions across the membrane pore as a continuous-time stochastic dynamical system that satisfies Langevin's equation.
2) We then carry out a probabilistic analysis of the dynamics of the ions. We show that the multiple ions propagating via the Langevin equation achieve a stationary distribution (steady-state) exponentially fast (Theorem 1). For Brownian dynamics simulation to yield a statistically valid estimate of the ion channel current, it is essential for the system to achieve stationarity at an exponential rate. We show that the current flowing through the ion channel can be formulated in terms of mean first passage times of ions (Theorem 3)—and these mean first passage times satisfy a boundary valued partial differential equation.
3) Because the partial differential equation for the mean first passage times cannot be solved explicitly, it is necessary to solve it numerically via Brownian dynamics simulation. We present the Brownian dynamics simulation algorithm as a randomized (stochastic simulation) algorithm for solving this partial differential equation, yielding statistically consistent estimates of these passage times and hence the ion channel current. We show the statistical consistency of the current obtained from the Brownian dynamics simulation algorithm (Theorem 4). More specifically, this theorem shows that the simulated current converges to the solution of the partial differential equation.
4) With the above foundation, we present a novel adaptive controlled Brownian dynamics simulation for estimating the PMF of the ion channel. The algorithm controls the interacting multiparticle Brownian dynamical system and yields a provably convergent estimate of PMF profile of the nanotube for any arbitrary ion channel. We show in numerical examples implemented on a supercomputer that for gramicidin-A ion channels, the controlled Brownian dynamics simulation yields the PMF profile estimate that is consistent with other methods.

B. Context and Background

Brownian Dynamics Simulation: In modeling biological ion channels, Brownian dynamics (BD) so far has proved to be a powerful tool, directly linking macroscopic observables to the atomic details of the protein macromolecules through the fundamental processes operating in electrolyte solutions. Because water molecules are ubiquitous in biological systems, their explicit modeling is usually very costly. The effect of the surrounding water molecules that form the bulk of the system is represented in BD by an average frictional and random force via a functional central limit theorem approximation. An implicit treatment of water in this way reduces the simulation time of an assembly consisting of the channel protein and spherical ions in the reservoirs by many orders of magnitude. Also, the atoms forming the channel are assumed to be rigid. With these two simplifying assumptions, it is possible to calculate conductance of an ion channel.

One-dimensional Brownian dynamics was introduced by Jakobsson and coworkers for the gramicidin channel and potassium channel [5], [6]. More recently, 3-D BD has been widely used for modeling biological ion channels incorporating a large reservoir attached to each end of the channel. This 3-D semimicroscopic simulation technique has been widely applied to study the permeation dynamics in a range of physiological systems, such as the KcsA potassium channel [7], calcium channels [8], gramicidin-A channel [3], and porin [9]. These studies provide detailed information about mechanisms underlying the permeation of ions across the nanotubes formed by the protein walls—see also [2] for further details.

Gramicidin-A ion channels: We illustrate the performance of the controlled Brownian dynamics simulation algorithm on gramicidin-A ion channels in this paper. Gramicidin-A is an antibiotic produced by *Bacillus brevis* [10, pp. 130]. Since the structure of gramicidin-A ion channels are simple, well known and have been studied in great detail, they form a useful benchmark for theoretical models that seek to explain how ions conducted through a cell membrane cause ion channel currents. Another reason why we consider gramicidin-A ion channels is that their radius is much smaller than other biological ion channels. As a result, it has been recently been shown that the determination of the PMF by solving Poisson's equation does not yield accurate results that fit experimental data [3]. Poisson's equation assumes that the ion is a point charge and therefore works well in wide ion channels where the size of the ion relative to the ion channel radius does not play a significant role. However, in gramicidin-A ion channels, the channel is

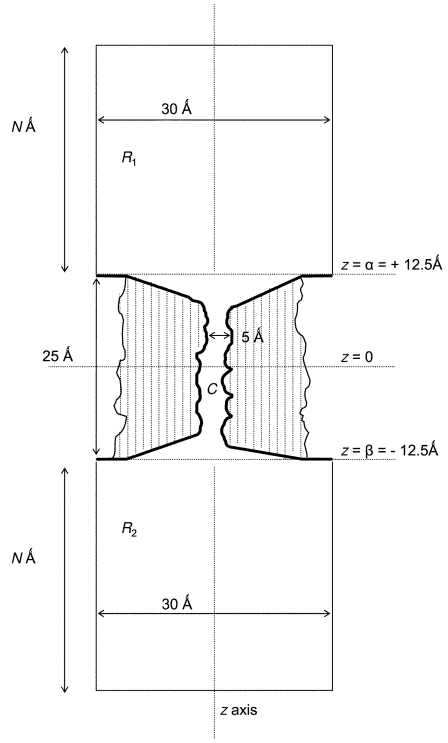

Fig. 1. Simulation assembly composed of gramicidin-A (hatched) and two cylindrical reservoirs $\mathcal{R}_1$, $\mathcal{R}_2$ containing $2N$ ions. The ion conducting path is denoted as $\mathcal{C}$.

very narrow and comparable to the size of the ions. As a result the point charge assumption breaks down. The charges appear as finite dimensional particles. Furthermore also due to the mesoscopic nature of the gramicidin-A ion channel, molecular dynamics do not yield a satisfactory fit to experimental data [11].

II. Brownian Dynamics Simulation Model of Gramicidin-A Ion Channel

In this section, we formulate a BD simulation model for a gramicidin-A ion channel at a mesoscopic time scale.

A. Permeation Model of Gramicidin-A Ion Channel

All the atoms forming an ion channel are placed in the center of the simulation assembly. The channel protein is assumed to have a rigid structure corresponding to the average positions of atoms forming it. Despite this necessary simplification imposed on the model, it has been shown previously that BD captures the salient conduction properties of a number of ion channels. This is because the most essential features that govern the permeation of ions across a narrow pore are captured in the model. There are minor details that can be neglected in the model for the purpose of BD simulations. For example, small variations in the radius of the ion conducting pathway have no perceptible effects on electrostatic calculations and BD results. In contrast, such variations would have a drastic effect on molecular dynamics results. To carry out BD simulations of ion channels, one needs to specify the boundaries of the system.

Fig. 1 shows a schematic illustration of a simulation assembly for a generalized ion channel. The ion channel, shown here as a cylindrical tube with irregular boundaries, is placed at the center of the assembly. We use the atomic coordinates stored in the Protein Data Bank with accession code IMAG. To define the surface of the channel, and hence the dielectric boundary, the radii of atoms in the gramicidin peptide are required. We used the same radii as in [3]. The gramidicin dimer is embedded in a neutral membrane of length 33 A, modeled as a uniform dielectric medium (with dielectric constant equal to that of the gramicidin peptide) without any charges or dipoles. The atoms forming the ion channel are represented as a homogeneous medium with a dielectric constant of 2 (shaded area in Fig. 1). Then, a large reservoir with a fixed number of K^+ (or Na^+) and Cl^- ions is attached at each end of the ion channel. The electrolyte in the two reservoirs comprises 55 M of implicit water and 150-mM concentrations of K^+ and Cl^- ions. The dielectric constants of the reservoirs ($\mathcal{R}_1$ and $\mathcal{R}_2$) and the interior of the ion channel $\mathcal{C}$ are assumed to be 80 and 60, respectively. The membrane potential is imposed by applying a uniform electric field across the ion channel. This is equivalent to placing a pair of large plates far away from the ion channel and applying a potential difference between the two plates. When an ion strikes the reservoir boundary during simulations, it is elastically scattered back into the reservoir. This operation is equivalent to letting an ion enter the reservoir whenever one leaves the simulation system. Thus, the concentrations of ions in the reservoirs are maintained at the desired values at all times. During simulations of current measurements, the chosen concentration values in the reservoirs are maintained by recycling ions from one side to the other whenever there is an imbalance due to a conduction event.

The number of ions that must be placed in each reservoir for a chosen concentration depends on the size of the reservoir. Because the computational cost is proportional to the square of the number of ions in the simulation system, it is desirable to have a small reservoir. At the same time, it must be large enough such that the ions in the system are in conditions similar to those in bulk electrolyte solutions. For example, the number of ions near the entrance of the pore should fluctuate according to the binomial distribution. To meet these requirements, an elaborate treatment of boundaries using a grand canonical Monte Carlo method was proposed [9]. Subsequently, [8] showed that, provided the dimensions of the reservoirs are about 3–4 Debye lengths, the simple stochastic boundary as described above gives the same results as the method proposed in [9].

The permeation model comprises $2N$ ions, where N denotes a positive integer. Throughout, we index the $2N$ ions by $i = 1, 2, \ldots, 2N$. These $2N$ ions comprise the following.

- N positive charged K^+ ions indexed by $i = 1, 2, \ldots, N$ initially placed in the reservoirs. Of these K^+ ions, $N/2$ ions indexed by $i = 1, 2, \ldots N/2$ are in $\mathcal{R}_1$ and $N/2$ ions indexed by $i = N/2 + 1, \ldots, 2N$ are in $\mathcal{R}_2$. Each K^+ ion has charge $q^{(i)} = q^+ = 1.6 \times 10^{-19}$ C, mass $m^{(i)} = m^+ = 6.5 \times 10^{-26}$ kg and frictional coefficient $m^+\gamma^+$, where from the Einstein–Smoluchowski relation

$$m^+\gamma^+ = \frac{kT}{D^+}, \quad D^+ = 1.96 \times 10^{-9}\ \mathrm{m}^2/\mathrm{s} \tag{1}$$

Here D^+ denotes the diffusion coefficient of the K^+ ion within a bulk solution. Also $k = 1.38 \times 10^{-23}$ J/T denotes

the Boltzmann constant and T denotes the temperature in Kelvin. K^+ ions have a radius $r^+ = 1.33$ Å. (Note: 1 Å (angstrom) $= 10^{-10}$ m).

- N negative charge Cl^- (Chloride) ions initially placed in the reservoirs. We index these by $i = N+1, N+2, \ldots, 2N$. Of these, $N/2$ Cl^- ions indexed by $i = N = 1, \ldots 3N/2$ are placed in $\mathcal{R}_1$ and the remaining $N/2$ Cl^- ions indexed by $i = 3N/2+1, \ldots, 2N$ are placed in $\mathcal{R}_2$. Each Cl^- ion has charge $q^{(i)} = q^- = -1.6 \times 10^{-19}$ C, mass $m^{(i)} = m^- = 5.9 \times 10^{-26}$ kg and frictional coefficient $m^-\gamma^- = kT/D^-$ where $D^- = 2.03 \times 10^{-9}$ m/s^2. Cl^- ions have a radius $r^- = 1.81$ Å.

The cylindrical reservoirs $\mathcal{R}_1$ and $\mathcal{R}_2$ in Fig. 1 are each 30 Å in radius and N Å in height. Specifying the height of each reservoir to be N Å guarantees that the concentration of ions in them is 300 mM. For example, the gramicidin-A ion channel $\mathcal{C}$ is modeled as cylindrical nanotube with diameter 4 Å and length 25 Å [3] that connects the two reservoirs. Thus, $\mathcal{R} = \mathcal{R}_1 \cup \mathcal{R}_2 \cup \mathcal{C}$ denotes the open set composed of the interior of the reservoirs and ion channel.

B. Mesoscopic Brownian Dynamics Model Formulation

Let $t \geq 0$ denote continuous time. Each ion i moves in 3-D space over time. Let $\mathbf{x}_t^{(i)} = (x_t^{(i)}, y_t^{(i)}, z_t^{(i)})' \in \mathcal{R}$ and $\mathbf{v}_t^{(i)} \in \mathbb{R}^3$ denote the position and velocity of ion i at time t. Here and throughout this paper all vectors are column vectors and denoted by the boldface font. Also we use $'$ to denote transpose of a vector or matrix. The three components $x_t^{(i)}$, $y_t^{(i)}$, $z_t^{(i)}$ of $\mathbf{x}_t^{(i)} \in \mathcal{R}$ are, respectively, the x, y, and z position coordinates. Similarly, the three components of $\mathbf{v}_t^{(i)} \in \mathbb{R}^3$ are the x, y, z velocity components.

At time $t = 0$, the position $\mathbf{x}_0^{(i)}$ and velocity $\mathbf{v}_0^{(i)}$ of each of the $2N$ ions in the two reservoirs are randomly initialized as follows: The upper reservoir is divided into N cells of equal volume. In each cell is placed either one K^+ or one Cl^- ion, each with probability half. The initial position $\mathbf{x}_0^{(i)}$ of ion i is chosen according to the uniform distribution within its cell. Similarly the remaining $N/2$ Na^+ ions $\{N/2+1, \ldots, N\}$ and remaining $N/2$ Cl^- ions $\{3N/2+1, \ldots, 2N\}$ are placed uniformly in the lower reservoir. This initialization of $\mathbf{x}_0^{(i)}$ emulates the BD computer software and also is necessary to ensure that two particles are not placed too close to each other. The initial velocity vectors $\mathbf{v}_0^{(i)}$ of the $2N$ ions are typically initialized according to a 3-D Gaussian distribution with zero mean, and 3×3 diagonal positive definite covariance matrix. Thus, the distribution of the magnitude of the initial velocity $|\mathbf{v}_0^{(i)}|$ has a Maxwell density.

From time $t = 0$ onwards, an external potential $\Phi_\lambda^{\text{ext}}(\mathbf{x})$ is applied along the z axis of Fig. 1, i.e., with $\mathbf{x} = (x, y, z)$

$$\Phi_\lambda^{\text{ext}}(\mathbf{x}) = -\mathbf{E}^{\text{ext}} z \tag{2}$$

where $-\mathbf{E}^{\text{ext}}$ is the external field in V/m in z direction. Applied potential λ is related to $\mathbf{E}^{\text{ext}}$ by $\mathbf{E}^{\text{ext}} = -\lambda/l$, where l is a length of the channel, and $\lambda \in \Lambda$. Here Λ denotes a finite set of applied experimental conditions such as applied voltages. For example,

$$\Lambda = \{-200, -180, \ldots, 0, \ldots, 180\,200\}\text{mV}. \tag{3}$$

Due to this applied external potential, the Na^+ ions drift from reservoir $\mathcal{R}_1$ to $\mathcal{R}_2$ via the ion channel $\mathcal{C}$ in Fig. 1.

Let $\mathbf{X}_t = (\mathbf{x}_t^{(1)\prime}, \mathbf{x}_t^{(2)\prime}, \mathbf{x}_t^{(3)\prime}, \ldots, \mathbf{x}_t^{(2N)\prime})' \in \mathcal{R}^{2N}$ denote the positions and $\mathbf{V}_t = (\mathbf{v}_t^{(1)\prime}, \mathbf{v}_t^{(2)\prime}, \mathbf{v}_t^{(3)\prime}, \ldots, \mathbf{v}_t^{(2N)\prime})' \in \mathbb{R}^{6N}$, denote the velocities of all the $2N$ ions at time $t \geq 0$. The position and velocity of each individual ion evolves according to the following continuous time stochastic dynamical system (recall $i = 1, 2, \ldots, N$ denote positive ions and $i = N+1, \ldots, 2N$ denote negative ions):

$$\mathbf{x}_t^{(i)} = \mathbf{x}_0^{(i)} + \int_0^t \mathbf{v}_s^{(i)} ds, \tag{4}$$

$$m^+\mathbf{v}_t^{(i)} = m^+\mathbf{v}_0^{(i)} - \int_0^t m^+\gamma^+\left(\mathbf{x}_s^{(i)}\right)\mathbf{v}_s^{(i)} ds + \int_0^t F_{\theta,\lambda}^{(i)}(\mathbf{X}_s) ds + b^+\left(\mathbf{x}_s^{(i)}\right)\mathbf{w}_t^{(i)} \tag{5}$$

$$m^-\mathbf{v}_t^{(i)} = m^-\mathbf{v}_0^{(i)} - \int_0^t m^-\gamma^-\left(\mathbf{x}_s^{(i)}\right)\mathbf{v}_s^{(i)} ds + \int_0^t F_{\theta,\lambda}^{(i)}(\mathbf{X}_s) ds + b^-\left(\mathbf{x}_s^{(i)}\right)\mathbf{w}_t^{(i)} \tag{6}$$

where $\gamma^\pm(\mathbf{x}_s^{(i)}) = \gamma^\pm$ [defined in (1)] if $\mathbf{x}_s^{(i)} \in \mathcal{R}_1 \cup \mathcal{R}_2$, i.e., if the ion is in the reservoir, and $\gamma(\mathbf{x}_s^{(i)})$ is determined by molecular dynamics simulation when the ion is in the ion channel [12]. Equation (4) merely says that velocity is the time derivative of the position. Equations (5) and (6) constitute the well-known *Langevin* equations. We now describe the various quantities in the above equations.

In (5) and (6), the process $\{\mathbf{w}_t^{(i)}\}$ denotes zero mean 3-D Brownian motion, which is component-wise independent. The terms $b^+(\mathbf{x}_s^{(i)})$ and $b^-(\mathbf{x}_s^{(i)})$ are, respectively

$$b^{+2}\left(\mathbf{x}_s^{(i)}\right) = 2m^+\gamma^+\left(\mathbf{x}_s^{(i)}\right)kT,$$
$$b^{-2}\left(\mathbf{x}_s^{(i)}\right) = 2m^-\gamma^-\left(\mathbf{x}_s^{(i)}\right)kT. \tag{7}$$

The noise processes $\{\mathbf{w}_t^{(i)}\}$ and $\{\mathbf{w}_t^{(j)}\}$, that drive any two different ions, $j \neq i$, are assumed statistically independent.

In (5) and (6), $F_{\theta,\lambda}^{(i)}(\mathbf{X}_t) = -q^{(i)}\nabla_{\mathbf{x}_t^{(i)}}\Phi_{\theta,\lambda}^{(i)}(\mathbf{X}_t)$ represents the *systematic force* acting on ion i, where the scalar valued process $\Phi_{\theta,\lambda}^{(i)}(\mathbf{X}_t)$ is the total electric potential experienced by ion i given the position $\mathbf{X}_t$ of the $2N$ ions. The subscript λ is the applied external potential in (2). The subscript θ is a parameter vector that characterizes the PMF, which is an important component of $\Phi_{\theta,\lambda}^{(i)}(\mathbf{X}_t)$. Later in this paper, we will present novel learning-based dynamic control algorithms for estimating θ given experimentally measured ion channel currents. For now, it may be assumed that θ is some constant finite dimensional

vector. As described below, $F^{(i)}_{\theta,\lambda}(\mathbf{X}_t)$ includes an ion-wall interaction force that ensures that position $\mathbf{x}^{(i)}_t$ of each ion lies in $\mathcal{R}$—see (11) below.

It is notationally convenient to represent the above system [(4), (5) and (6)] as a vector stochastic integral equation. Define the following vector valued variables:

$$\mathbf{V}_t = \begin{bmatrix} \mathbf{V}^+_t \\ \mathbf{V}^-_t \end{bmatrix}, \ \mathbf{V}^+_t = \begin{bmatrix} \mathbf{v}^{(1)}_t \\ \vdots \\ \mathbf{v}^{(N)}_t \end{bmatrix},$$

$$\mathbf{V}^-_t = \begin{bmatrix} \mathbf{v}^{(N+1)}_t \\ \vdots \\ \mathbf{v}^{(2N)}_t \end{bmatrix}, \ \zeta_t = \begin{bmatrix} \mathbf{X}_t \\ \mathbf{V}^+_t \\ \mathbf{V}^-_t \end{bmatrix},$$

$$\mathbf{F}^+_{\theta,\lambda}(\mathbf{X}_t) = \begin{bmatrix} \mathbf{F}^{(1)}_{\theta,\lambda}(\mathbf{X}_t) \\ \vdots \\ \mathbf{F}^{(N)}_{\theta,\lambda}(\mathbf{X}_t) \end{bmatrix}, \ \mathbf{F}^-_{\theta,\lambda}(\mathbf{X}_t) = \begin{bmatrix} \mathbf{F}^{(N+1)}_{\theta,\lambda}(\mathbf{X}_t) \\ \vdots \\ \mathbf{F}^{(2N)}_{\theta,\lambda}(\mathbf{X}_t) \end{bmatrix},$$

$$\mathbf{F}_{\theta,\lambda}(\mathbf{X}_t) = \begin{bmatrix} \frac{1}{m^+}\mathbf{F}^+_{\theta,\lambda}(\mathbf{X}_t) \\ \frac{1}{m^-}\mathbf{F}^-_{\theta,\lambda}(\mathbf{X}_t) \end{bmatrix}, \ \mathbf{f}_{\theta,\lambda}(\zeta_t) = \begin{bmatrix} \mathbf{0}_{6N\times 1} \\ \mathbf{F}_{\theta,\lambda}(\mathbf{X}_t) \end{bmatrix}. \quad (8)$$

The above system (4), (5), (6) can be written as the following vector stochastic dynamical system:

$$\zeta_t = \zeta_0 + \int_0^t \mathbf{A}(\mathbf{X}_\tau)\zeta_\tau d\tau + \int_0^t \mathbf{f}_{\theta,\lambda}(\zeta_\tau)d\tau + \int_0^t \Sigma^{1/2}(\mathbf{X}_\tau)\mathbf{w}_\tau d\tau \quad (9)$$

where
$\Sigma^{1/2}(\mathbf{X}_\tau) = \text{diag}(\mathbf{0}_{6N\times 6N}, b^+(\mathbf{X}_\tau)/m^+, b^-(\mathbf{X}_\tau)/m^-)$, $\mathbf{I}_{6N}$ denotes the $6N \times 6N$ identity matrix

$$\mathbf{w}_t = \begin{bmatrix} \mathbf{0}_{2N\times 1} \\ \mathbf{w}^{(1)}_t \\ \vdots \\ \mathbf{w}^{(2N)}_t \end{bmatrix},$$

$$\mathbf{A} = \left[\begin{array}{c|cc} \mathbf{0}_{6N\times 6N} & \multicolumn{2}{c}{\mathbf{I}_{6N}} \\ \hline \mathbf{0}_{6N\times 6N} & -\gamma^+(\mathbf{X}_\tau) & \mathbf{0}_{3N\times 3N} \\ & \mathbf{0}_{3N\times 3N} & -\gamma^-(\mathbf{X}_\tau) \end{array}\right]. \quad (10)$$

We will subsequently refer to (9) and (10) as the Brownian dynamics equations for a biological ion channel.

Remark: The BD approach is a stochastic averaging theory framework that models the average effect of water molecules:

1) The friction term $m\gamma\mathbf{v}^{(i)}_t dt$ captures the average effect of the ions driven by the applied external electrical field bumping into the water molecules every few femtoseconds. The frictional coefficient is given from Einstein's relation.
2) The Brownian motion term $\mathbf{w}^{(i)}_t$ also captures the effect of the random motion of ions bumping into water molecules and is given from the *fluctuation–dissipation* theorem.

C. Modeling of Systematic Force Acting on Ions

The systematic force experienced by each ion i is

$$F^{(i)}_{\theta,\lambda}(\mathbf{X}_t) = -q^{(i)}\nabla_{\mathbf{x}^{(i)}_t}\Phi^{(i)}_{\theta,\lambda}(\mathbf{X}_t)$$

where the scalar valued process $\Phi^{(i)}_{\theta,\lambda}(\mathbf{X}_t)$ denotes the total electric potential experienced by ion i given the position $\mathbf{X}_t$ of all the $2N$ ions. We now give a detailed formulation of these systematic forces.

The potential $\Phi^{(i)}_{\theta,\lambda}(\mathbf{X}_t)$ experienced by each ion i comprises the following five components:

$$\Phi^{(i)}_{\theta,\lambda}(\mathbf{X}_t) = U_\theta\left(\mathbf{x}^{(i)}_t\right) + \Phi^{\text{ext}}_\lambda\left(\mathbf{x}^{(i)}_t\right) + \Phi^{\text{IW}}\left(\mathbf{x}^{(i)}_t\right) + \Phi^{C,i}(\mathbf{X}_t) + \Phi^{SR,i}(\mathbf{X}_t). \quad (11)$$

Note that the first three terms in (11), namely, $U_\theta(\mathbf{x}^{(i)}_t)$, $\Phi^{\text{ext}}_\lambda(\mathbf{x}^{(i)}_t)$, $\Phi^{\text{IW}}(\mathbf{x}^{(i)}_t)$ depend only on the position $\mathbf{x}^{(i)}_t$ of ion i, whereas the last two terms in (11) $\Phi^{C,i}(\mathbf{X}_t)$, $\Phi^{SR,i}(\mathbf{X}_t)$ depend on the distance of ion i to all the other ions, i.e., the position $\mathbf{X}_t$ of all the ions. The five components in (11) are now defined.

1) PMF, denoted $U_\theta(\mathbf{x}^{(i)}_t)$ in (11), comprises electric forces acting on ion i when it is in or near the ion channel (nanotube $\mathcal{C}$ in Fig. 1). The PMF U_θ is a smooth function of the ion position $\mathbf{x}^{(i)}_t$ and depends on the structure of the ion channel. The main aim of controlled Brownian dynamics simulation algorithm proposed in Section V of this paper is to estimate the PMF $U_\theta(\cdot)$.

   The PMF U_θ originates from two different sources. First, there are fixed charges in the channel protein and the electric field emanating from them renders the pore attractive to one ionic species and repulsive to another. Some of the amino acids forming the ion channels carry the unit or partial electronic charges.

   Second, when any of the ions in the assembly comes near the protein wall, it induces surface charges of the same polarity at the water-protein interface. This is known as the induced surface charges. To understand the origin of these induced surface charges, consider a K^+ ion placed in a solution. Water molecules near the ion align themselves such that the oxygen atoms, with their partial negative charges positioned nearest to the ion. Each water molecule has a strong dipole moment of 1.84 Debye. Polar or carbonyl groups on the protein wall cannot rotate as freely as water molecules, and therefore at the water-protein interface, there are excesses of hydrogen atoms. These excess hydrogen atoms at the boundary appear as surface charges.
2) *External Applied Potential*: In the vicinity of living cells, there is a strong electric field resulting from the membrane potential, which is generated by diffuse, unpaired, ionic clouds on each side of the membrane. Typically, this resting potential across a cell membrane, whose thickness is about 50 Å, is 70 mV, the cell interior being negative with respect to the extracellular space. In simulations, this field is mimicked by applying a uniform electric field across the channel. Because the reservoirs are filled with electrolyte solutions, each reservoir is in iso-potential, and the potential drop occurs across the channel conduit.

   For ion i at position $\mathbf{x}^{(i)}_t = \mathbf{x} = (x, y, z)$, $\Phi^{\text{ext}}_\lambda(\mathbf{x}) = \lambda z$ [see (2)] denotes the potential on

ion i due to the applied external field. The electrical field acting on each ion due to the applied potential is therefore $-\nabla_{\mathbf{x}_t^{(i)}}\Phi_\lambda^{\text{ext}}(\mathbf{x}) = (0,0,\lambda)$ V/m at all $\mathbf{x} \in \mathcal{R}$. It is this applied external field that causes a drift of ions from the reservoir $\mathcal{R}_1$ to $\mathcal{R}_2$ via the ion channel $\mathcal{C}$. As a result of this drift of ions within the electrolyte in the two reservoirs, eventually the measured potential drop across the reservoirs is zero and all the potential drop occurs across the ion channel.

3) *Interion Coulomb Potential*: In (11), $\Phi^{C,i}(\mathbf{X}_t)$ denotes the Coulomb interaction between ion i and all the other ions.

$$\Phi^{C,i}(\mathbf{X}_t) = \frac{1}{4\pi\epsilon_0}\sum_{j=1,j\neq i}^{2N}\frac{q^{(j)}}{\epsilon_w\left\|\mathbf{x}_t^{(i)}-\mathbf{x}_t^{(j)}\right\|}. \tag{12}$$

4) *Ion-Wall Interaction Potential*: The ion-wall potential Φ^{IW}, also called the $(\sigma/r)^9$ potential, ensures that the position $\mathbf{x}_t^{(i)}$ of all ions $i = 1,\ldots,2N$ lie in $\mathcal{R}^o$. With $\mathbf{x}_t^{(i)} = (x_t^{(i)}, y_t^{(i)}, z_t^{(i)})'$, it is modeled as

$$\Phi^{\text{IW}}\left(\mathbf{x}_t^{(i)}\right) = \frac{F_0}{9}\frac{\left(r^{(i)}+r_w\right)^9}{\left[r_c+r_w-\left(\sqrt{\left(x_t^{(i)^2}+y_t^{(i)^2}\right)}\right)\right]^9} \tag{13}$$

where for positive ions $r^{(i)} = r^+$ (radius of Na^+ atom) and for negative ions $r^{(i)} = r^-$ (radius of Cl^- atom), $r_w = 1.4$ Å is the radius of atoms making up the wall, r_c denotes the radius of the ion channel, and $F_0 = 2\times 10^{-10}$ N which is estimated from the ST2 water model used in molecular dynamics. This ion-wall potential results in short range forces that are only significant when the ion is close to the wall of the reservoirs $\mathcal{R}_1$ and $\mathcal{R}_2$ or anywhere in the ion channel $\mathcal{C}$ (since the narrow segment of an ion channel can be comparable in radius to the ions).

5) *Short-Range Potential*: Finally, at short ranges, the Coulomb interaction between two ions is modified by adding a potential $\Phi^{SR,i}(\mathbf{X}_t)$, which replicates the effects of the overlap of electron clouds. Thus

$$\Phi^{SR,i}(\mathbf{X}_t) = \frac{F_0}{9}\sum_{j=1,j\neq i}^{2N}\frac{\left(r^{(i)}+r^{(j)}\right)}{\left\|\mathbf{x}_t^{(i)}-\mathbf{x}_t^{(j)}\right\|^9}. \tag{14}$$

Similar to the ion-wall potential, $\Phi^{SR,i}$ is significant only when ion i gets very close to another ion. It ensures that two opposite charge ions attracted by interion Coulomb forces (12) cannot collide and annihilate each other. Molecular dynamics simulations show that the hydration forces between two ions add further structure to the $1/|\mathbf{x}_t^{(i)}-\mathbf{x}_t^{(j)}||^9$ repulsive potential due to the overlap of electron clouds in the form of damped oscillations [13], [14]. [8] incorporated the effect of the hydration forces in (14) in such a way that the maxima of the radial distribution functions for $Na^+ - Na^+$, $Na^+ - Cl^-$ and $Cl^- - Cl^-$ would correspond to the values obtained experimentally.

III. Formulation of PMF Estimation Problem

Our goal is to estimate the PMF U_θ of a gramicidin-A ion channel. As mentioned in Section I, estimating U_θ gives useful information about the structure of the ion channel. In this section, we first present a Gaussian mixture basis function approximation of the PMF U_θ that is characterized by a five-dimensional (5-D) parameter vector θ. Then we formulate the PMF estimation problem as a stationary stochastic optimization problem. Section III-B gives a theoretical foundation to show that the stationary stochastic optimization problem is well posed, i.e., that the $2N$ particle system (9) eventually attains a stationary distribution. In Section IV, we given an explicit construction of how the simulated current (denoted $\hat{I}_T(\theta,\lambda)$ below) through the ion channel can be computed via BD simulation. Finally, in Section V-A, we formulate the problem of estimating the PMF U_θ as a stochastic optimization problem involving minimizing the mean square error between the BD simulated current ($\hat{I}_T(\theta,\lambda)$) and the actual observed experimental current I.

A. Gaussian Mixture Parameterization of Potential Mean Force (PMF)

In this subsection we propose a Gaussian basis function approximation to the PMF $U_\theta(\mathbf{x})$ of a gramicidin-A ion channel. The PMF structure of a gramicidin-A ion channel is well known [11]. Hence, a basis function approximation of the gramicidin-A PMF $U_\theta(\mathbf{x})$ needs to capture the following important properties of the gramicidin-A ion channel.

1) The ion moves strictly along the center of the ion channel, i.e., its coordinates $\mathbf{x} = (x,y,z) = (0,0,z)$. The PMF $U_\theta(\mathbf{x})$ (where $\mathbf{x} = (0,0,z)$) experienced by the ion within the gramicidin-A ion channel is symmetric with respect to z, i.e.,

$$U_\theta(\mathbf{x}) = U_\theta(0,0,z) = U_\theta(0,0,-z) \quad \text{for all } \mathbf{x} \in \mathcal{C}.$$

2) For $z < -20$ Å or $z > 20$ Å, i.e., in either reservoir at more than 20 Å from the center ($z = 0$) of the ion channel, $U_\theta(,z)$ should be close to zero—since the PMF only acts on ions in or near the ion channel.

Since the PMF $U_\theta(\mathbf{x})$ is a continuously differentiable function of $\mathbf{x}$, it can be uniformly approximated arbitrary closely by a set of Gaussian basis functions or some other radial basis function. By using physiological data of a gramicidin-A ion channel, we found that the following scaled Gaussian mixture comprising a linear combination of three Gaussian density functions gives an excellent fit:

$$U_\theta([0,0,z]) = m\exp\left(-\frac{1}{2}\frac{(z-W)^2}{\sigma^2}\right) + m\exp\left(-\frac{1}{2}\frac{(z+W)^2}{\sigma^2}\right) + m_0\exp\left(-\frac{1}{2}\frac{z^2}{\sigma_0^2}\right). \tag{15}$$

The above Gaussian mixture is parameterized by the 5-D parameter vector

$$\theta = \left(W, \sigma^2, m, \sigma_0^2, m_0\right)'. \tag{16}$$

The above Gaussian mixture comprises two Gaussian functions with identical weighting factors m and identical variance σ^2, centered about $z = W$ and $z = -W$, respectively—and a third zero mean Gaussian centered about $z = 0$ with variance σ_0^2 and weighting factor m_0. It is obvious that the above parameterization satisfies the symmetry property 1 above. Also for suitable choice of the parameter vector θ in (16), property 2 holds.

The structure of the gramicidin-A ion channel, implies that the parameters θ defined in (16) need to constrained to the set Θ defined as follows:

$$\Theta = \{\theta : W \in [0, 30\ \text{Å}], \sigma^2 \in \left[0, \sigma_{\max}^2\right], m \in [0, M], \\ \sigma_0^2 \in \left[0, \sigma_{\max}^2\right], m_0 \in [0, M]\} \tag{17}$$

where M and $\sigma_{\max}$ are positive bounded constants.

By using physiological data of a gramicidin-A ion channel, we computed the parameter θ^* that best fits the curve (15) to the physiological data (in terms of a least squares fit). This physiological data shows that for a gramicidin-A ion channel, U_θ has two potential wells of 7 kT along the z-axis, one at $z = -9$ Å, the other at $z = 9$ Å. Also at $z = 0$, the potential barrier is 5 kT (with respect to the potential wells). Using the Nelder–Mead simplex (direct search) optimization algorithm in Matlab, we obtained the best least squares fit over the interval $z \in [-20\ \text{Å}, 20\ \text{Å}]$ as

$$\theta^* = (9.00, 16.00, -7.11, 12.25, -1.41)'. \tag{18}$$

Fig. 2 shows the PMF generated by the Gaussian mixture approximation (15) with parameter θ^*.

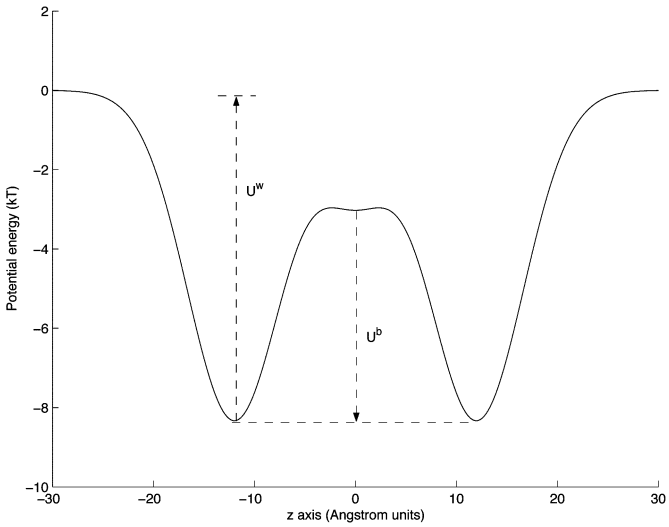

Fig. 2. PMF U_θ of gramicidin-A ion channel obtained by a three-component Gaussian mixture. The two basic parameters characterizing $U_\theta([0, 0, z])$ are the depths of the two well U^w and the height of the barrier U^b. The width of the barrier is approximately 10 Å. The PMF shown with $U^w = 8$ kT and $U^b = 5$ kT gives the best description of the physiological data on gramicidin-A ion channels.

B. Probabilistic Characterization of Ion Channel Current in Terms of Mean Passage Time

Thus far (9), (10), and (11) give a complete description of the stochastic dynamics of the ions. In addition, there are two key requirements that the BD dynamical simulation should take into account:

1. **Physiological concentration constraint**: The concentration of ions in each reservoir $\mathcal{R}_1$ and $\mathcal{R}_2$ should remain approximately constant and equal to the physiological concentration. Note that if the system was allowed to evolve for an infinite time with the channel open, then eventually due to the external applied potential, more ions will be in $\mathcal{R}_2$ than $\mathcal{R}_1$, This would violate the condition that the concentration of particles in $\mathcal{R}_1$ and $\mathcal{R}_2$ remain constant.
2. **Two-time scale constraint**: The dynamics of the BD simulation has an inherent two-time scale property. Typically the time for an ion to enter and propagate through the ion channel is at least an order of magnitude larger compared to the time it takes for an ions to move within a reservoir. That is the time constant for the particles in the reservoirs to attain steady state is much smaller than the time it takes for a particle to enter and propagate through the channel.

The following two-step probabilistic construction formalizes the above two requirements and ensures that they are satisfied.

Procedure 1: **Probabilistic construction of Brownian dynamics ion permeation in ion channel**

1) *Step 1*: The $2N$ ions in the system are initialized as described before in (2) and the ion channel $\mathcal{C}$ is closed. The system evolves and attains stationarity. Theorem 1 below shows that the probability density function of the $2N$ particles converges exponentially fast to a unique stationary distribution. Theorem 2 shows that in the stationary regime, all positive ions in reservoir $\mathcal{R}_1$ have the same stationary distribution and so are statistically indistinguishable (similarly for $\mathcal{R}_2$).
2) *Step 2*: After stationarity is achieved, the ion channel is opened. The ions evolve according to (9). As soon as an ion from $\mathcal{R}_1$ crosses the ion channel $\mathcal{C}$ and enters $\mathcal{R}_2$, the experiment is stopped. Similarly if an ion from $\mathcal{R}_2$ crosses $\mathcal{C}$ and enters $\mathcal{R}_1$, the experiment is stopped. Theorem 3 gives partial differential equations for the mean time an ion in $\mathcal{R}_1$ takes to cross the ion channel and reach $\mathcal{R}_2$ (and for the time it takes an ion to cross from $\mathcal{R}_2$ to $\mathcal{R}_1$). From this a theoretical expression for the mean ion channel current is constructed (25).

Remark: The above construction is a mathematical idealization. In actual BD algorithms, the ion channel is kept open and ions that cross the channel are simply removed and replaced in their original reservoir. However, as described later (following Algorithm 1), the above mathematical construction is an excellent approximation due to the fact that by virtue of Step 1, the system of particles with the newly replaced ion converges exponentially fast to its stationary distribution, and by virtue of the two-time scale property, the time taken to attain this stationary

distribution is much smaller than the time it takes for a single ion to cross the ion channel.

Let $\pi_t^{(\theta,\lambda)}(\mathbf{X},\mathbf{V})$ denote the joint probability density function of the position and velocity of all the $2N$ ions at time $t \geq 0$. We explicitly denote the θ, λ dependence of the probability density functions, since they depend on the PMF U_θ and applied external potential λ. Note that the marginal probability density function $\pi_t^{(\theta,\lambda)}(\mathbf{X}) = p^{(\theta,\lambda)}(\mathbf{x}_t^{(1)}, \mathbf{x}_t^{(2)}, \ldots, \mathbf{x}_t^{(2N)})$ of the positions of all $2N$ ions at time t is obtained as

$$\pi_t^{(\theta,\lambda)}(\mathbf{X}) = \int_{\mathbb{R}^{6N}} \pi_t^{(\theta,\lambda)}(\mathbf{X},\mathbf{V}) d\mathbf{V}.$$

The following result proved in the appendix states that for the above stochastic dynamical system, $\pi_t^{(\theta,\lambda)}(\mathbf{X},\mathbf{V})$ converges exponentially fast to its stationary (invariant) distribution $\pi_\infty^{(\theta,\lambda)}(\mathbf{X},\mathbf{V})$. That is, the ions in the two reservoirs attain steady state exponentially fast.

Theorem 1: Consider Step 1 of the Brownian dynamics probabilistic construction in Procedure 1. For the Brownian dynamics system, represented in (9) and (10), comprising $2N$ ions, with $\zeta = (\mathbf{X},\mathbf{V})$, there exists a unique stationary distribution $\pi_\infty^{(\theta,\lambda)}(\zeta)$, and constants $K > 0$ and $0 < \rho < 1$, such that

$$\sup_{\zeta \in \mathcal{R}^{2N} \times \mathbb{R}^{6N}} \left| \pi_t^{(\theta,\lambda)}(\zeta) - \pi_\infty^{(\theta,\lambda)}(\zeta) \right| \leq K \mathcal{V}(\zeta) \rho^t \tag{19}$$

Here $\mathcal{V}(\zeta) > 1$ is a measurable function on $\mathcal{R}^{2N} \times \mathbb{R}^{6N}$.

Proof: We show below that the system when all the ions are in the reservoirs (Step 1 of probabilistic construction Section III-B) is V-uniform ergodic. This implies exponential ergodicity (see, for details, [15]). To prove V-uniform ergodicity, we invoke the following sufficient condition for V-uniform ergodicity [15]; ζ_t is V-uniform ergodic if there exists a twice differentiable Lyapunov function $\mathcal{V}(\zeta) > 1$ such that

$$\mathcal{L}\mathcal{V} \leq -c\mathcal{V} + d\mathbf{1}_{Q_0} \tag{20}$$

for positive constants c and d, and some compact nonempty set Q_0. Here $\mathcal{L}$ denotes the backward operator defined in (29), $\mathbf{1}_{Q_0}$ denotes the indicator function for the set Q_0, i.e., $\mathbf{1}_{Q_0} = 1$ if $\zeta \in Q_0$ and 0 otherwise, and $\mathcal{L}$ is defined in (29). For our Brownian dynamics model (9), when all ions are in the reservoir, $\gamma^\pm$ and hence $b^\pm$ and A are constants; see discussion below (6). The following choice of $\mathcal{V}$ satisfies (20):

$$\mathcal{V}(\mathbf{X},\mathbf{V}) = \frac{1}{2}\mathbf{V}'\mathbf{V} + \sum_{i=1}^{2N} \Phi_{\theta,\lambda}^{(i)}(\mathbf{X}) + 1. \tag{21}$$

■

The next result to establish is, under the conditions of Step 1, the ions in the two reservoirs are statistically indistinguishable. Denote the stationary marginal density of ion i as $\pi_\infty^{(\theta,\lambda)}(\mathbf{x}^{(i)},\mathbf{v}^{(i)})$.

Theorem 2: Consider Step 1 of the Brownian dynamics probabilistic construction in Procedure 1. Then all the positive ions in reservoir $\mathcal{R}_1$ have identical stationary marginal density and all negative ions in $\mathcal{R}_1$ have identical stationary marginal density. The same result hold for $\mathcal{R}_2$.

Theorem 2 is not surprising—as (4), (5), and (6) are symmetric in i, one would intuitively expect that once steady state as been attained, all the positive ions behave identically—similarly with the negative ions. Due to the above result, once the system has attained steady state, any positive ion is representative of all the N positive ions, and similarly for the negative ions.

Having described the main theorems of Step 1, we now proceed to Step 2 of the BD construction of Procedure 1. Assume that the system (9) comprising $2N$ ions has attained stationarity with the ion channel $\mathcal{C}$ closed according to Step 1. Now in Step 2 of Procedure 1, the ion channel is opened so that ions can diffuse into it. Our key result below is to give a boundary valued partial differential equation for the mean passage time for an ion to cross the ion channel—this immediately yields an equation for the ion channel current.

Let $\tau_{\mathcal{R}_1,\mathcal{R}_2}^{(\theta,\lambda)}$ denote the "mean first passage time" for any of the $N/2$ K^+ ions in $\mathcal{R}_1$ to travel to $\mathcal{R}_2$ via the channel $\mathcal{C}$, and $\tau_{\mathcal{R}_2,\mathcal{R}_1}^{(\theta,\lambda)}$ denote the minimum time for any of the $N/2$ K^+ ions in $\mathcal{R}_2$ to travel to R_1

$$\tau_{\mathcal{R}_1,\mathcal{R}_2}^{(\theta,\lambda)} = \mathbf{E}\{t_\beta\}, \quad \tau_{\mathcal{R}_2,\mathcal{R}_1}^{(\theta,\lambda)} = \mathbf{E}\{t_\alpha\} \tag{22}$$

where

$$\begin{aligned} t_\beta &\triangleq \inf\left\{t : \max\left(z_t^{(1)}, z_t^{(2)}, \ldots, z_t^{(N/2)}\right) \geq \beta\right\}, \\ t_\alpha &\triangleq \inf\left\{t : \min\left(z_t^{(N/2+1)}, z_t^{(N/2+2)}, \ldots, z_t^{(2N)}\right) \leq \alpha\right\}. \end{aligned} \tag{23}$$

In cationic channels, for example, only K^+ or Na^+ ions flow through to cause the channel current—so we do not need to consider the mean passage time of the Cl^- ions. To give a partial differential equation for $\tau_{\mathcal{R}_1,\mathcal{R}_2}^{(\theta,\lambda)}$ and $\tau_{\mathcal{R}_2,\mathcal{R}_1}^{(\theta,\lambda)}$, it is convenient to define the closed sets

$$\begin{aligned} \mathcal{P}_2 &= \left\{\zeta : \left\{z^{(1)} \geq \beta\right\} \cup \left\{z^{(2)} \geq \beta\right\} \cup \cdots \cup \left\{z^{(N/2)} \geq \beta\right\}\right\} \\ \mathcal{P}_1 &= \left\{\zeta : \left\{z^{(N/2+1)} \leq \alpha\right\} \cup \cdots \cup \left\{z^{(2N)} \leq \alpha\right\}\right\}. \end{aligned} \tag{24}$$

Then it is clear that $\zeta_t \in \mathcal{P}_2$ is equivalent to $\max(z_t^{(1)}, z_t^{(2)}, \ldots, z_t^{(N/2)}) \geq \beta$, since either expression implies that at least one ion has crossed from $\mathcal{R}_1$ to $\mathcal{R}_2$. Similarly, $\zeta_t \in \mathcal{P}_1$ is equivalent to $\min(z_t^{(N/2+1)}, z_t^{(N/2+2)}, \ldots, z_t^{(2N)}) \leq \alpha$. Thus, t_β and t_α defined in (23) can be expressed as $t_\beta = \inf\{t : \zeta_t \in \mathcal{P}_2\}$, $t_\alpha = \inf\{t : \zeta_t \in \mathcal{P}_1\}$.

In terms of the mean first passage times $\tau_{\mathcal{R}_1,\mathcal{R}_2}^{(\theta,\lambda)}, \tau_{\mathcal{R}_2,\mathcal{R}_1}^{(\theta,\lambda)}$ defined in (23), the mean current flowing from $\mathcal{R}_1$ via the ion channel $\mathcal{C}$ into $\mathcal{R}_2$ is defined as

$$I^{(\theta,\lambda)} = q^+ \left(\frac{1}{\tau_{\mathcal{R}_1,\mathcal{R}_2}^{(\theta,\lambda)}} - \frac{1}{\tau_{\mathcal{R}_2,\mathcal{R}_1}^{(\theta,\lambda)}} \right). \tag{25}$$

In Section IV we show that this current can be estimated by counting the number of ions going thorough the ion channel via a Brownian dynamics simulation.

The following result adapted from [16, pp. 306] shows that the mean passage times $\tau^{(\theta,\lambda)}_{\mathcal{R}_1,\mathcal{R}_2}$ and $\tau^{(\theta,\lambda)}_{\mathcal{R}_2,\mathcal{R}_1}$ satisfy boundary valued partial differential equations. In particular, the expressions for the mean passage time below together with (25) give a complete characterization of the ion channel current. Of course, the partial differential equation cannot be solved in closed form—so later on in this paper we use BD simulation as a randomized numerical method for solving this partial differential equation.

Theorem 3: Consider the two-step BD probabilistic construction in Procedure 1. Then the mean first passage times $\tau^{(\theta,\lambda)}_{\mathcal{R}_1,\mathcal{R}_2}$ and $\tau^{(\theta,\lambda)}_{\mathcal{R}_2,\mathcal{R}_1}$ [defined in (25)] for ions to diffuse through the ion channel are obtained as

$$\tau^{(\theta,\lambda)}_{\mathcal{R}_1,\mathcal{R}_2} = \int\limits_{\Xi_{\mathcal{R}_1}} \tau^{(\theta,\lambda)}_{\mathcal{R}_1,\mathcal{R}_2}(\zeta)\pi^{(\theta,\lambda)}_{\infty}(\zeta)d\zeta \tag{26}$$

$$\tau^{(\theta,\lambda)}_{\mathcal{R}_2,\mathcal{R}_1} = \int\limits_{\Xi_{\mathcal{R}_2}} \tau^{(\theta,\lambda)}_{\mathcal{R}_2,\mathcal{R}_1}(\zeta)\pi^{(\theta,\lambda)}_{\infty}(\zeta)d\zeta \tag{27}$$

where

$$\tau^{(\theta,\lambda)}_{\mathcal{R}_1,\mathcal{R}_2}(\zeta) = \mathbf{E}\left\{\inf\{t : \zeta_t \in \mathcal{P}_2 | \zeta_0 = \zeta\}\right\},$$
$$\tau^{(\theta,\lambda)}_{\mathcal{R}_2,\mathcal{R}_1}(\zeta) = \mathbf{E}\left\{\inf\{t : \zeta_t \in \mathcal{P}_1 | \zeta_0 = \zeta\}\right\}.$$

Here $\tau^{(\theta,\lambda)}_{\mathcal{R}_1,\mathcal{R}_2}(\zeta)$ and $\tau^{(\theta,\lambda)}_{\mathcal{R}_2,\mathcal{R}_1}(\zeta)$ satisfy the following boundary value partial differential equations

$$\mathcal{L}\left(\tau^{(\theta,\lambda)}_{\mathcal{R}_1,\mathcal{R}_2}(\zeta)\right) = -1 \;\; \zeta \notin \mathcal{P}_2, \;\; \tau^{(\theta,\lambda)}_{\mathcal{R}_1,\mathcal{R}_2}(\zeta) = 0 \;\; \zeta \in \mathcal{P}_2$$
$$\mathcal{L}\left(\tau^{(\theta,\lambda)}_{\mathcal{R}_2,\mathcal{R}_1}(\zeta)\right) = -1 \;\; \zeta \notin \mathcal{P}_1, \;\; \tau^{(\theta,\lambda)}_{\mathcal{R}_2,\mathcal{R}_1}(\zeta) = 0 \;\; \zeta \in \mathcal{P}_1 \tag{28}$$

where for any test function $\phi(\cdot)$, $\mathcal{L}$ denotes the backward elliptic operator (infinitesimal generator)

$$\mathcal{L}(\phi) = \frac{1}{2}\mathrm{Tr}\left[\Sigma\nabla^2_{\zeta}\phi(\zeta)\right] + \left(\mathbf{f}_{\theta,\lambda}(\zeta) + \mathbf{A}\zeta\right)' \nabla_{\zeta}\phi(\zeta). \tag{29}$$

Furthermore, $\tau^{(\theta,\lambda)}_{\mathcal{R}_1,\mathcal{R}_2}$ and $\tau^{(\theta,\lambda)}_{\mathcal{R}_2,\mathcal{R}_1}$ are finite.

IV. Brownian Dynamics Simulation for Estimation of Ion Channel Current

It is not possible to solve the boundary valued PDEs (28) to obtain explicit closed form expressions. The aim of BD simulation is to obtain estimates of these quantities by directly simulating the stochastic dynamical system (9). Thus, BD simulation can be viewed as a simulation based (randomized) numerical method for solving this partial differential equation.

A. Time Discretization of Ion Dynamics

To implement the BD simulation algorithm described below on a digital computer, it is necessary to discretize the continuous-time dynamical equation (9) of the $2N$ ions. A two-time scale time discretization is used in the BD simulation algorithm. For dynamics of ions within the ion channel, the BD simulation algorithm uses a sampling interval of $\Delta = 2 \times 10^{-15}$ s. For dynamics of ions within the reservoirs a sampling interval of $\Delta = 10^{-13}$ s is used in the reservoirs. These choices of Δ are based on extensive numerical testing of the BD simulation algorithm. There are several possible methods for time discretization of the stochastic differential equation (9); see [17]. Our BD simulation algorithm uses the second-order discretization approximation of [18].

B. Brownian Dynamics Simulation Algorithm

In the BD simulation Algorithm 1 below, we use the following notation.

The algorithm runs for L iterations where L is user specified. Each iteration l, $l = 1, 2, \ldots, L$, runs for a random number of discrete-time steps until an ion crosses the channel. We denote these random times as $\hat{\tau}^{(l)}_{\mathcal{R}_1,\mathcal{R}_2}$ if the ion has crossed from $\mathcal{R}_1$ to $\mathcal{R}_2$ and $\hat{\tau}^{(l)}_{\mathcal{R}_2,\mathcal{R}_1}$ if the ion has crossed from $\mathcal{R}_2$ to $\mathcal{R}_1$. Thus

$$\hat{\tau}^{(l)}_{\mathcal{R}_1,\mathcal{R}_2} = \min\left\{k : \zeta^{(d)}_k \in \mathcal{P}_2\right\},$$
$$\hat{\tau}^{(l)}_{\mathcal{R}_2,\mathcal{R}_1} = \min\left\{k : \zeta^{(d)}_k \in \mathcal{P}_1\right\}.$$

The positive ions $\{1, 2, \ldots, N/2\}$ are in $\mathcal{R}_1$ at steady state $\pi^{\theta,\lambda}_{\infty}$, and the positive ions $\{N/2+1, \ldots, 2N\}$ are in $\mathcal{R}_2$ at steady state.

$L_{\mathcal{R}_1,\mathcal{R}_2}$ is a counter that counts how many K^+ ions have crossed from $\mathcal{R}_1$ to $\mathcal{R}_2$ and $L_{\mathcal{R}_2,\mathcal{R}_1}$ counts how many K^+ ions have crossed from $\mathcal{R}_2$ to $\mathcal{R}_1$. Note $L_{\mathcal{R}_1,\mathcal{R}_2} + L_{\mathcal{R}_2,\mathcal{R}_1} = L$.

In the algorithm below, to simply notation, we only consider passage of K^+ ions $i = 1, \ldots, N$ across the ion channel.

Algorithm 1: **Brownian Dynamics Simulation Algorithm (for fixed θ and λ)**

- Input parameters θ for PMF and λ for applied external potential.
- For $l = 1$ to L iterations:
  - — *Step 1.* Initialize all $2N$ ions according to stationary distribution $\pi^{(\theta,\lambda)}_{\infty}$.
    Open ion channel at discrete time $k = 0$ and set $k = 1$.
  - — *Step 2.* Propagate all $2N$ ions according to the time discretized Brownian dynamical system until time k^* at which an ion crosses the channel.
    - If ion crossed ion channel from $\mathcal{R}_1$ to $\mathcal{R}_2$, i.e., for any ion $i^* \in \{1, 2, \ldots, N/2\}$, $z^{(i^*)}_{k^*} \geq \beta$ then set $\hat{\tau}^{(l)}_{\mathcal{R}_1,\mathcal{R}_2} = k^*$.
      Update number of crossings from $\mathcal{R}_1$ to $\mathcal{R}_2$: $L_{\mathcal{R}_1,\mathcal{R}_2} = L_{\mathcal{R}_1,\mathcal{R}_2} + 1$.
    - If ion crossed ion channel from $\mathcal{R}_2$ to $\mathcal{R}_1$, i.e., for any ion $i^* \in \{N/2+1, \ldots, N\}$, $z^{(i)}_{k^*} \leq \alpha$ then set $\hat{\tau}^{(l)}_{\mathcal{R}_2,\mathcal{R}_1} = k^*$.
      Update number of crossings from $\mathcal{R}_2$ to $\mathcal{R}_1$: $L_{\mathcal{R}_2,\mathcal{R}_1} = L_{\mathcal{R}_2,\mathcal{R}_1} + 1$.
  - — End for loop.

- Compute the mean first passage time and mean current estimate after L iterations as

$$\hat{\tau}^{(\theta,\lambda)}_{\mathcal{R}_1,\mathcal{R}_2}(L) = \frac{1}{L_{\mathcal{R}_1,\mathcal{R}_2}} \sum_{l=1}^{L_{\mathcal{R}_1,\mathcal{R}_2}} \hat{\tau}^{(l)}_{\mathcal{R}_2,\mathcal{R}_1},$$

$$\hat{\tau}^{(\theta,\lambda)}_{\mathcal{R}_2,\mathcal{R}_1}(L) = \frac{1}{L_{\mathcal{R}_2,\mathcal{R}_1}} \sum_{l=1}^{L_{\mathcal{R}_2,\mathcal{R}_1}} \hat{\tau}^{(l)}_{\mathcal{R}_2,\mathcal{R}_1}, \tag{30}$$

$$\hat{I}^{(\theta,\lambda)}(L) = q^+\left(\frac{1}{\hat{\tau}^{(\theta,\lambda)}_{\mathcal{R}_1,\mathcal{R}_2}(L)} - \frac{1}{\hat{\tau}^{(\theta,\lambda)}_{\mathcal{R}_2,\mathcal{R}_1}(L)}\right). \tag{31}$$

The following result shows that the estimated current $\hat{I}^{\theta,\lambda}(L)$ obtained from a BD simulation run over L iterations is strongly consistent.

Theorem 4: For fixed PMF $\theta \in \Theta$ and applied external potential $\lambda \in \Lambda$ (3) the ion channel current estimate $\hat{I}^{\theta,\lambda}(L)$ obtained from the BD simulation Algorithm 1 over L iterations is strongly consistent, i.e., $\lim_{L\to\infty} \hat{I}^{\theta,\lambda}(L) = I^{(\theta,\lambda)}$ w.p. 1 where $I^{(\theta,\lambda)}$ is the mean current defined in (25).

Proof: Since by construction in Algorithm 1, each of the L iterations are statistically independent, and $\mathbf{E}\{\hat{\tau}^{(l)}_{\mathcal{R}_1,\mathcal{R}_2}\}$, $\mathbf{E}\{\hat{\tau}^{(l)}_{\mathcal{R}_2,\mathcal{R}_1}\}$ are finite (see Theorem 3), it then follows by Kolmogorov's strong law of large numbers

$$\lim_{L\to\infty} \hat{\tau}^{(\theta,\lambda)}_{\mathcal{R}_1,\mathcal{R}_2}(L) = \tau^{(\theta,\lambda)}_{\mathcal{R}_1,\mathcal{R}_2}, \quad \lim_{L\to\infty} \hat{\tau}^{(\theta,\lambda)}_{\mathcal{R}_2,\mathcal{R}_1}(L) = \tau^{(\theta,\lambda)}_{\mathcal{R}_2,\mathcal{R}_1} \text{ w.p.1.}$$

Thus $q^+(1/\hat{\tau}^{(\theta,\lambda)}_{\mathcal{R}_1,\mathcal{R}_2}(L) - 1/\hat{\tau}^{(\theta,\lambda)}_{\mathcal{R}_2,\mathcal{R}_1}(L)) \to I^{(\theta,\lambda)}$ w.p. 1 as $L \to \infty$. ∎

Implementation Details and Variations of Algorithm 1: Algorithm 1 is an idealization where all ions are reset to $\pi^{(\theta,\lambda)}_\infty$ in Step 1 when any ion crosses the channel. In our actual numerical implementation of the BD simulation the following approximation of Algorithm 1 was used. Instead of Step 2b and 3b, only remove the crossed ion denoted as i^* and put it back in its reservoir with the stationary marginal probability—see Theorem 2. The other particles are not reset. Since as described in the probabilistic construction above, the time it takes for the ions in the reservoir to attain steady state is much faster than the time for an ion to cross the channel, the above approximation does not affect the statistical properties of the BD simulation (such as mean passage time).

V. Controlled Brownian Dynamics Mesoscopic Simulation of Gramicidin-A Ion Channel

We will estimate the PMF U_θ parameterized by θ, by computing the θ that optimizes the fit between the mean current $I^{(\theta,\lambda)}$ [defined above in (25)] and the experimentally observed current $y(\lambda)$ defined below. Unfortunately, it is impossible to explicitly compute $I^{(\theta,\lambda)}$ from (25). For this reason we resort to a *stochastic optimization problem formulation* below, where consistent estimates of $I^{(\theta,\lambda)}$ are obtained via the Brownian dynamics simulation Algorithm 1. The main algorithm presented in this section is the controlled Brownian Dynamics Simulation Algorithm 2 which solves the stochastic optimization problem and yields the optimal PMF.

A. Formulation of PMF Estimation as Stochastic Optimization Problem

Suppose that the BD simulation Algorithm 1 is run in batches indexed by batch number $n = 1, 2, \ldots$. In each batch n, the PMF parameter θ_n is selected (as described below), an external potential $\lambda \in \Lambda$ is applied, and the BD Algorithm 1 is run over L iterations, and the estimated current $\hat{I}^{(\theta,\lambda)}_n$ is computed using (31). From experimental data, an accurate estimate of the current–voltage concentration profiles of an ion channel can be obtained. These curves depict the actual current $y(\lambda)$ flowing through an ion channel for various external applied potentials $\lambda \in \Lambda$ and ionic concentrations. For fixed applied field $\lambda \in \Lambda$ at a given concentration, define the square error loss function for the nth batch as

$$\mathcal{Q}_n(\theta,\lambda) = \left(\hat{I}^{(\theta,\lambda)}_n - y(\lambda)\right)^2 \tag{32}$$

and the expected loss functions

$$\mathcal{Q}(\theta,\lambda) = \mathbf{E}\left\{\mathcal{Q}_n(\theta,\lambda)\right\}, \quad \mathcal{Q}(\theta) = \sum_{\lambda\in\Lambda} \mathcal{Q}(\theta,\lambda).$$

Note that the total loss function $\mathcal{Q}(\theta)$ is obtained by adding the square error over all the applied fields $\lambda \in \Lambda$ on the current-voltage or current-concentration curve. The optimal PMF U_{θ^*} is determined by the parameter θ^* that minimizes the above loss function: $\theta^* = \arg\min_{\theta\in\Theta} \mathcal{Q}(\theta)$.

B. Stochastic Gradient Algorithms for Estimating PMF and the Need for Gradient Estimation

We now give a complete description of the controlled Brownian dynamics simulation algorithm for computing the optimal PMF estimate U_{θ^*}. The algorithm is schematically depicted in Fig. 3. Recall $n = 0, 1, \ldots$, denotes batch number.

Algorithm 2: Controlled Brownian Dynamics Simulation Algorithm for Estimating PMF

- *Step 0*: Set batch index $n = 0$, and initialize $\theta_0 \in \Theta$.
- *Step 1 (Evaluation of Loss Function)*: At batch n, evaluate loss function $\mathcal{Q}_n(\theta_n,\lambda)$ for each external potential $\lambda \in \Lambda$.
- *Step 2 (Gradient Estimation)*: Compute gradient estimate $\widehat{\nabla}_\theta \mathcal{Q}_n(\theta_n,\lambda)$ either as a finite difference (35) below, or according to the SPSA algorithm (see discussion below).
- *Step 3 (Stochastic Approximation Algorithm)*: Update PMF estimate

$$\theta_{n+1} = \theta_n - \epsilon_{n+1} \sum_{\lambda\in\Lambda} \widehat{\nabla}_\theta \mathcal{Q}_n(\theta_n,\lambda) \tag{33}$$

  where ϵ_n denotes a decreasing step size (see discussion below for choice of step size).
- Set n to $n+1$ and go to Step 1.

A crucial aspect of the above algorithm is the gradient estimation Step 2. In this step, an estimate $\widehat{\nabla}_\theta \mathcal{Q}_n(\theta,\lambda)$ of the gradient $\nabla_\theta \mathcal{Q}_n(\theta,\lambda)$ is computed. This gradient estimate is then

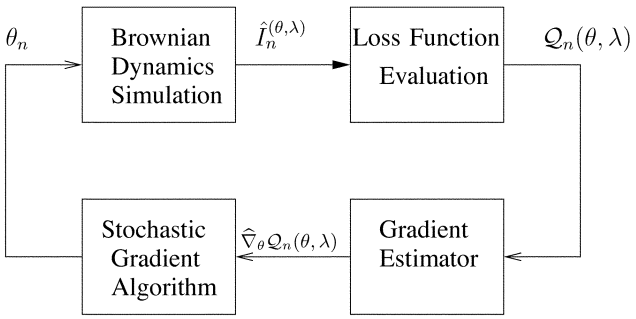

Fig. 3. Controlled Brownian dynamics simulation for estimating PMF.

fed to the stochastic gradient algorithm (Step 3) which updates the PMF. Note that since the explicit dependence of $\mathcal{Q}_n(\theta,\lambda)$ on θ is not known, it is not possible to compute $\nabla_\theta \mathcal{Q}_n(\theta,\lambda)$. Thus, we have to resort to gradient estimation.

Choice of Step Size: The step size ϵ_n is typically chosen as

$$\epsilon_n = \epsilon/(n+1+R)^\kappa \tag{34}$$

where $0.5 < \kappa \leq 1$ and R is some positive constant. This choice of step size satisfies the condition $\sum_{n=1}^{\infty} \epsilon_n = \infty$, which is required for convergence of Algorithm 2.

Kiefer–Wolfowitz Finite Difference Gradient Estimator: An obvious gradient estimator is obtained by finite differences as follows. Suppose θ is a p dimensional vector. Let $\mathbf{e}_1, \mathbf{e}_2, \ldots, \mathbf{e}_p$ denote p dimensional unit vectors, where e_i is a unit vector with 1 in the ith position and zeros elsewhere. Then the two-sided finite difference gradient estimator is

$$\widehat{\nabla}_\theta \mathcal{Q}_n(\theta,\lambda) = \begin{bmatrix} \frac{\mathcal{Q}_n(\theta_n+\mu_n\mathbf{e}_1,\lambda)-\mathcal{Q}_n(\theta_n-\mu_n\mathbf{e}_1,\lambda)}{2\mu_n} \\ \frac{\mathcal{Q}_n(\theta_n+\mu_n\mathbf{e}_2,\lambda)-\mathcal{Q}_n(\theta_n-\mu_n\mathbf{e}_2,\lambda)}{2\mu_n} \\ \vdots \\ \frac{\mathcal{Q}_n(\theta_n+\mu_n\mathbf{e}_p,\lambda)-\mathcal{Q}_n(\theta_n-\mu_n\mathbf{e}_p,\lambda)}{2\mu_n} \end{bmatrix}. \tag{35}$$

Using (35) in Algorithm 2 yields the so-called finite difference stochastic gradient algorithm.

The main disadvantages of the above finite gradient estimator are twofold. First, the bias of the gradient estimate is $O(\mu_n^2)$. Second, the simulation cost of implementing the above estimator is large. It requires $2p$ BD simulations, since two BD simulations are required to evaluate $\mathcal{Q}_n(\theta_n + \mu_n\mathbf{e}_i,\lambda)$ and $\mathcal{Q}_n(\theta_n - \mu_n\mathbf{e}_i,\lambda)$ for each $i = 1,2,\ldots,p$.

Remark: Instead of the Kiefer–Wolfowitz algorithm, the simultaneous perturbation stochastic approximation (SPSA) algorithm [19] is a novel method that picks a single random direction $\mathbf{d}_n$ along which direction the derivative is evaluated at each batch n. Thus, SPSA only requires two BD simulations per iteration, i.e., the number of evaluations is independent of the dimension p of the parameter vector θ. We refer the reader to [19] and the SPSA Web site.[1] There are other more sophisticated gradient estimators that can be implemented—such as weak derivative estimators and infinitesimal perturbation analysis (IPA) estimators; see [20].

[1][Online]. Available: http://www.jhuapl.edu/SPSA/

Convergence of Controlled Brownian Dynamics Simulation Algorithm 2: The estimates θ_n generated by Algorithm 2 (whether using the Kiefer–Wolfowitz or SPSA algorithm) converge to a local minimum of the loss function.

Theorem 5: For batch size $L \to \infty$ in Algorithm 1, the sequence of estimates $\{\theta_n\}$ generated by the controlled Brownian dynamics simulation Algorithm 2, converge at $n \to \infty$ to a the locally optimal PMF estimate θ^* with probability one.

Since by construction of the BD algorithm, for fixed θ, $\mathcal{Q}_n(\theta,\lambda)$ are independent and identically distributed (i.i.d.) random variables, the proof of the above theorem involves showing strong convergence of a stochastic gradient algorithm with i.i.d. observations—which is quite straightforward. In [21, Theorem 4.3, Sec. 8.4], almost sure convergence of stochastic gradient algorithms for state dependent Markovian noise under general conditions is presented.

VI. Simulation Experiments for Gramicidin-A Ion Channel

The controlled Brownian dynamics simulation Algorithm 2 was run on the Australian Partnership for Advanced Computing (APAC) Linux cluster supercomputer for estimating the PMF U_θ of a gramicidin-A ion channel. This is a 800-Gflop supercomputer comprising 152 Dell Precision 350 Linux nodes, with each node being a 2.65-GHz Pentium 4.

Consider the parameterization $\theta = (W, \sigma^2, m, \sigma_0^2, m_0)'$ defined in (16) for the PMF U_θ. Since the position of the potential wells for a gramicidin-A ion channel are precisely known to be at -9 Å and 9 Å, we fixed the components $W = 9$, $\sigma^2 = 16$, and $\sigma_0^2 = 12.25$ in θ. Our aim is to estimate the two components $\theta = (m, m_0)$ which determines the depth of the two potential wells of a gramicidin-A ion channel and the height of the potential barrier between the wells. This is obtained by estimating the parameter θ^* that optimizes the fit between the BD simulated current and experimentally determined current. The experimentally determined current $y(\lambda)$ was evaluated at five voltages $\lambda \in \Lambda = \{1.9, 2, 3.2, 4, 5\}$ pA on the *I–V* curve of a gramicidin-A ion channel.

The controlled BD simulation Algorithm 2 was run to estimate θ^*. The Kiefer–Wolfowitz finite difference method (35) was used in Algorithm 2 to estimate the PMF parameter $\theta = (m, m_0)$. The step size chosen for the Kiefer–Wolfowitz estimator (35) was $\mu = 0.2$, $\gamma = 0.5$, $\mu_k = \mu/(k+1)^\gamma$. The step size chosen for the stochastic gradient algorithm (34) was $\epsilon = 0.002$, $\kappa = 1$. The algorithm was initialized with $\theta_0 = [-6, -3]$.

Fig. 4 shows the evolution of the estimates $\{\theta_k\}$ versus batch index $k = 0, 1 \ldots$, generated by the controlled BD Algorithm 2. Each iteration (batch) took approximately 3 h on the supercomputer. It can be seen that the estimates converge within 60 batches (iterations). The estimate $\theta_{60} = (-7.09, -1.41)$. In Fig. 5 we plot the PMF U_{θ_0} for parameter θ_0 that was used to initialize Algorithm 2. This PMF U_{θ_0} has potential wells of depth 6 kT and potential barrier of 3 kT. In Fig. 5, we also plot the PMF estimate $U_\theta(\theta_{60})$ obtained after 60 batches of running Algorithm 2. It is seen from Fig. 5 that the PMF estimate $U_\theta(\theta_{60})$ has a potential well of depth $U^w = 7.1$ kT and potential barrier $U^b = 4.6$ kT. The well depth here refers to the zero potential in

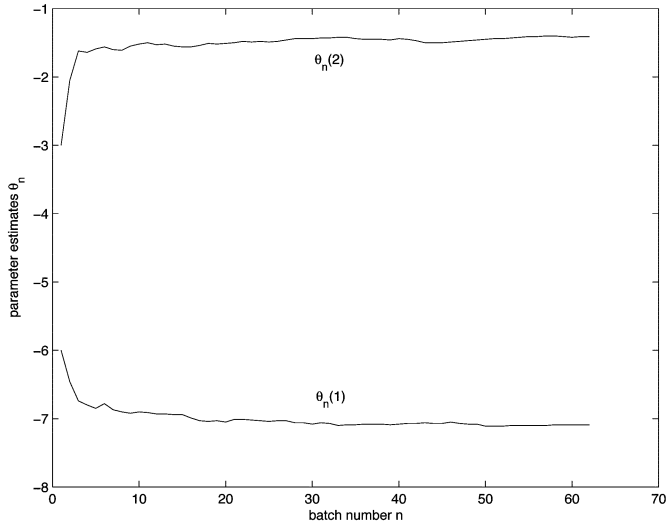

Fig. 4. Evolution of PMF parameter estimates θ_n for gramicidin-A ion channel generated by controlled Brownian dynamics simulation algorithm 2. The algorithm was run on the ANU supercomputer and the Kiefer–Wolfowitz gradient estimator was used.

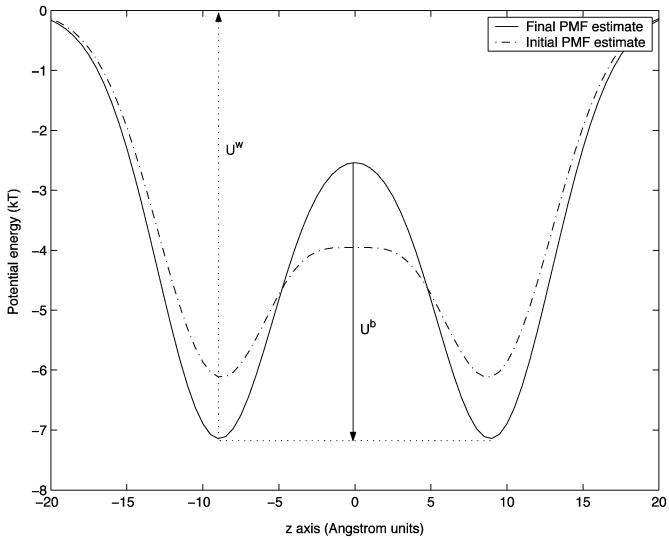

Fig. 5. PMF U_θ for initial parameter estimate θ_0 and final parameter estimate θ_{60} for gramicidin-A channel. The final parameter estimate yields the PMF estimate for gramicidin-A has two potential wells of depth $U^w = -7.14$ kT and potential barrier $U^b = 4.61$ kT.

the reservoir and the barrier height is measured with respect to the well minimum. Previously, [3] estimated the shape of the potential profile for K^+ ions using the brute-force inverse method. The depth of the wells and the height of the barrier they quote are, respectively, 8 kT and 5 kT. It is of interest to compare these profiles with those of [5]. In [5], the conductance properties of Na^+ ions were replicated via electrodiffusion equations using a profile with the well depth of 5.4 kT and the barrier height of 4.2 kT. Reference [22] also shows that similar well depths and barrier heights are required to match experimental conductances using their diffusion theory. Thus, the previous estimates of the parameters set, obtained by using a variety of different methods, are congruent to those obtained with the PMF estimate obtained from the novel controlled Brownian dynamics algorithm proposed in this paper.

VII. Conclusions and Extensions

The approach of this paper can be generalized to other ion channels. For example, in ion channels with larger radius than gramicidin-A, the ions can be considered as point masses and the force experienced by an ion at any position can be computed by solving Poisson's equation numerically. However, solving Poisson's equation involves assigning the dielectric constants of the water-filled pore and the protein, as well as the prior knowledge of the magnitudes of charges carried by polar and ionizable residues in the protein. Instead, by using the techniques in this paper it is possible to directly compute the optimum PMF (i.e., estimate the solution to Poisson's equation) that best fits the experimental ion channel current. In our recent work, we have used globally convergent discrete stochastic search algorithms to verify that the above simulation results are accurate.

References

[1] V. Krishnamurthy and S. Chung, "Brownian dynamics simulation for modeling ion permeation across bio-nanotubes," *IEEE Trans. NanoBiosci.*, vol. 4, no. 1, pp. 102–111, Mar. 2005.

[2] S. Chung, O. Andersen, and V. Krishnamurthy, *Handbook of Biological Membrane Ion Channels: Dynamics, Structure and Applications*. New York: Springer-Verlag, 2006.

[3] S. Edwards, B. Corry, S. Kuyucak, and S. Chung, "Continuum electrostatics fails to describe ion permeation in the gramicidin channel," *Biophys. J.*, vol. 83, pp. 1348–1360, Sep. 2002.

[4] M. O'Mara, P. H. Barry, and S. H. Chung, "A model of the glycine receptor deduced from Brownian dynamics studies," *Proc. Nat. Acad. Sci. USA*, vol. 100, pp. 4310–4315, 2003.

[5] S. Chiu and E. Jakobsson, "Stochastic theory of singly occupied ion channels. II. Effects of access resistance and potential graidents extending into the bath," *Biophys. J.*, vol. 55, pp. 147–157, 1989.

[6] S. Bek and E. Jakobsson, "Brownian dynamics study of a multiply occupied cation channel: application to understanding permeation in potassium channel," *Biophys. J.*, vol. 66, pp. 1028–1038, 1994.

[7] T. Allen and S. Chung, "Brownian dynamics study of an open-state KcsA potassium channel," *Biochim. Biophys. Acta—Biomembranes*, vol. 1515, pp. 83–91, 2001.

[8] B. Corry, S. Kuyucak, and S. Chung, "Tests of continuum theories as models of ion channels. II. Poisson-Nernst-Planck theory versus Brownian dynamics," *Biophys. J.*, vol. 78, pp. 2364–2381, May 2000.

[9] W. Im and B. Roux, "Ions and counterions in a biological channel: A molecular dynamics simulation of OmpF porin from escherichia coli in an explicit membrane with 1 M KCl aqueous salt solution," *J. Mol. Biol.*, vol. 319, pp. 1177–1197, 2002.

[10] A. Finkelstein, *Water Movement Through Lipid Bilayers, Pores and Plasma Membranes*. New York: Wiley-Interscience, 1987.

[11] T. W. Allen, T. Bastug, S. Kuyucak, and S. H. Chung, "Gramicidin A channel as a test ground for molecular dynamics force fields," *Biophys. J.*, vol. 84, pp. 2159–2168, 2003.

[12] T. W. Allen, S. Kuyucak, and S. H. Chung, "Molecular dynamics estimates of ion diffusion in model hydrophobic and KcsA potassium channels," *Biophys. Chem.*, vol. 86, pp. 1–14, 2000.

[13] E. Guärdia, R. Rey, and J. Padrö, "Potential of mean force by constratined molecular dynamics: A sodium chloride ion-pair in water," *Chem. Phys.*, vol. 155, pp. 187–195, 1991.

[14] ——, " $Na^+ - Na^+$ and $Cl^- - Cl^-$ ion pairs in water: mean force potentials by constrained molecular dynamics," *J. Chem. Phys.*, vol. 95, pp. 2823–2831, 1991.

[15] S. P. Meyn and R. L. Tweedie, "Stability of Markovian processes III: Foster–Lyapunov criteria for continuous time processes," *Adv. Appl. Probability*, vol. 25, pp. 518–548, 1993.

[16] I. Gihman and A. Skorohod, *Stochastic Differential Equations*. New York: Springer-Verlag, 1972.

[17] P. E. Kloeden and E. Platen, *Numerical Solution of Stochastic Differential Equations*. Berlin, Germany: Springer-Verlag, 1992.

[18] W. v. Gunsteren, H. Berendsen, and J. Rullmann, "Stochastic dynamics for molecules with constraints Brownian dynamics of n-alkalines," *Mol. Phys.*, vol. 44, no. 1, pp. 69–95, 1981.
[19] J. Spall, *Introduction to Stochastic Search and Optimization*. New York: Wiley, 2003.
[20] G. Pflug, *Optimization of Stochastic Models: The Interface Between Simulation and Optimization*. Norwell, MA: Kluwer Academic, 1996.
[21] H. Kushner and G. Yin, *Stochastic Approximation Algorithms and Recursive Algorithms and Applications*, 2nd ed. New York: Springer-Verlag, 2003.
[22] P. McGill and M. Schumaker, "Boundary conditions for single-ion diffusion," *Biophys. J.*, vol. 71, pp. 1723–1742, 1996.

Vikram Krishnamurthy (S'90-M'91-SM'99-F'05) was born in 1966. He received the B.S. degree in electrical engineering from the University of Auckland, New Zealand, in 1988 and the Ph.D. degree from the Australian National University, Canberra, in 1992.

He was a Chaired Professor at the Department of Electrical and Electronic Engineering, University of Melbourne, Australia, where he also served as Deputy Head of Department. Since 2002, he has been a Professor and Canada Research Chair at the Department of Electrical Engineering, University of British Columbia, Vancouver, BC, Canada. He has served as Associate Editor for *Systems and Control Letters* and *European Journal of Applied Signal Processing*. His research interests span several areas, including ion channels and nanobiology, stochastic scheduling and control, statistical signal processing, and wireless telecommunications.

Dr. Krishnamurthy has served as Associate Editor for the IEEE TRANSACTIONS ON SIGNAL PROCESSING, the IEEE TRANSACTIONS ON AEROSPACE AND ELECTRONIC SYSTEMS, and the IEEE TRANSACTIONS ON CIRCUITS AND SYSTEMS—II. He was guest editor of a special issue of IEEE TRANSACTIONS ON NANOBIOSCIENCE in March 2005 on bionanotubes.

Shin-Ho Chung received B.Sc. degrees from Stanford University, Stanford, CA, and London University, London, U.K., and the Ph.D. degree from Harvard University, Cambridge, MA.

He held a postdoctoral position at the Research Laboratory of Electronics, Massachusetts Institute of Technology, Cambridge. Currently, he is the Head of the Biophysics Group in the Department of Theoretical Physics, Australian National University, Canberra. His primary research effort is aimed at building theoretical models of biological ion channels.